



HAL
open science

Model-order reduction for nonlinear dynamics including nonlinearities induced by damage

Alexandre Daby-Seesaram, Amélie Fau, Pierre-Étienne Charbonnel, David Néron

► **To cite this version:**

Alexandre Daby-Seesaram, Amélie Fau, Pierre-Étienne Charbonnel, David Néron. Model-order reduction for nonlinear dynamics including nonlinearities induced by damage. 6th ECCOMAS Young Investigators Conference, Jul 2021, Valence, Spain. 10.4995/YIC2021.2021.13255 . hal-03654222

HAL Id: hal-03654222

<https://hal.science/hal-03654222>

Submitted on 28 Apr 2022

HAL is a multi-disciplinary open access archive for the deposit and dissemination of scientific research documents, whether they are published or not. The documents may come from teaching and research institutions in France or abroad, or from public or private research centers.

L'archive ouverte pluridisciplinaire **HAL**, est destinée au dépôt et à la diffusion de documents scientifiques de niveau recherche, publiés ou non, émanant des établissements d'enseignement et de recherche français ou étrangers, des laboratoires publics ou privés.

Model-order reduction for nonlinear dynamics including nonlinearities induced by damage

Alexandre Daby-Seesaram^{*†}, Amélie Fau^{*}, Pierre-Étienne Charbonnel[†] and David Néron^{*}

^{*} Université Paris-Saclay, ENS Paris-Saclay, CNRS, LMT
Laboratoire de Mécanique et Technologie, 91190, Gif-sur-Yvette, France
{alexandre.daby-seesaram, amelie.fau, david.neron}@ens-paris-saclay.fr

[†] DES - Service d'Études Mécaniques et Thermiques (SEMT), CEA, Université Paris-Saclay,
91191 Gif-sur-Yvette, France
pierreetienne.charbonnel@cea.fr

Key words: LATIN-PGD, model-order reduction, damage, fragility curves, seismic risk assessment

Abstract: *Assessing the probability of failure of a structure under seismic loading requires the simulation of a great number of similar nonlinear computations. A model-order reduction strategy is proposed for decreasing the computational cost associated to each nonlinear simulation. In this contribution, the method is illustrated to evaluate the damage evolution in a primary circuit piping component of a pressurized water reactor, subjected to accidental seismic input. Piping components are described with a damageable elasto-plastic material exhibiting a preliminary damage pattern.*

1 INTRODUCTION

Fragility curves are one of the main tools for characterizing the resistance of civil engineering structures, such as nuclear facilities, to seismic hazard. These curves describe the probability that the response of a structure exceeds a given criterion, called “failure criterion”, as a function of the expected seismic loading level. Their computational cost is expensive as a large number of loading scenarii must be considered to model seismic input variability, but also due to the inherent uncertainties (material parameters, geometry, modelling errors, etc.) that must be taken into account for reliability assessment. Their construction therefore falls into the scope of the *many-queries* problems where the need to reduce the numerical cost of each simulation is imperative. Another point is that the final aim of the study is to add a preliminary structural damage as a parameter of those charts. Decreasing the computational costs of solving large dimensional problems has long been studied and decreasing the dimension of the solution space has shown to be of great interest. Among the several existing methods, one finds *Model-Order Reduction* (MOR) techniques. Some of them (referred to as *a posteriori* methods) require beforehand the computation of a given reduced basis, while others (referred to as *a priori* methods) consist in building the reduced basis simultaneously with the computation. The first kind, including among others the use of Ritz vectors [1] or the Proper Orthogonal Decomposition (POD) [2], has greatly been studied in [3] where a wide range of reduced basis choices have been examined. In this last reference, computation time saving and robustness of the basis considered are looked over. It highlights that the choice of the basis proves to be decisive and when dealing with numerous computations, finding an ideal reduced basis on which to project the solutions to these various problems may not be an obvious task. To overcome this difficulty it is relevant to build the reduced basis on-the-fly, as the solver progresses, to optimize the choice of new modes. Such *a priori* model-order reduction methods include the *Proper Generalized*

Decomposition (PGD) [4] which is used in the present work.

Herein, the focus is on the implementation of a strategy based on *a priori* model-order reduction for the calculation of the nonlinear dynamics problem at stake. Among the different possible approaches, the PGD coupled with the LATIN method [5] is particularly well suited for solving parameterized problems in nonlinear mechanics in order to build numerical charts [6]. The LATIN-PGD method is an iterative approach that seeks the solution of a given problem by building, in a greedy way, a dedicated reduced-order basis. This basis can be reused and enriched, allowing a good numerical efficiency. It has been applied to solve a wide range of problems in mechanics (and more recently for earthquake-engineering applications [7]). Here we develop this method to solve the low-frequency dynamics problem that arises when applying seismic loading to metallic piping structures with a nonlinear behaviour while taking into account their possibly pre-damaged state.

2 DYNAMIC EQUATIONS

The spatial domain on which the problem is written is denoted Ω . On that body of density ρ , body forces \mathbf{f}_d and surface forces \mathbf{F}_d are applied on Ω and on $\partial\Omega_2$ respectively while imposed displacements u_d are applied on $\partial\Omega_1$ as described in Fig. 1.

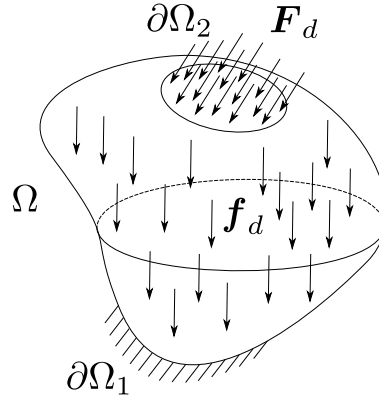


Figure 1: Reference problem on the domain Ω

Let us then define the three sets defining *admissibility*:

- $\mathcal{U} = \left\{ \mathbf{u} \mid \varepsilon(\mathbf{u}) = \frac{1}{2} (\nabla \mathbf{u} + {}^T \nabla \mathbf{u}), \dot{\mathbf{u}}|_{t=0} = \mathbf{0}, \mathbf{u}|_{t=0} = \mathbf{0} \text{ in } \Omega, \right.$
 $\left. \mathbf{u} = \mathbf{u}_d \text{ on } \partial\Omega_1 \text{ and } \dot{\mathbf{u}} = \dot{\mathbf{u}}_d \text{ on } \partial\Omega_1 \right\},$
- $\mathcal{U}^0 = \left\{ \mathbf{u} \mid \varepsilon(\mathbf{u}) = \frac{1}{2} (\nabla \mathbf{u} + {}^T \nabla \mathbf{u}), \dot{\mathbf{u}}|_{t=0} = \mathbf{0}, \mathbf{u}|_{t=0} = \mathbf{0} \text{ in } \Omega, \right.$
 $\left. \mathbf{u} = \mathbf{0} \text{ on } \partial\Omega_1 \text{ and } \dot{\mathbf{u}} = \mathbf{0} \text{ on } \partial\Omega_1 \right\},$
- $\mathcal{S} = \left\{ \boldsymbol{\sigma} \mid \nabla \cdot \boldsymbol{\sigma} + \mathbf{f}_d = \rho \ddot{\mathbf{u}} \text{ in } \Omega \text{ and } \boldsymbol{\sigma} \mathbf{n} = \mathbf{F}_d \text{ on } \partial\Omega_2 \right\},$

\mathcal{U} (respectively \mathcal{U}^0) is the kinematically admissible (respectively to zero) displacements set and \mathcal{S} is the dynamically admissible stress set. $\boldsymbol{\sigma}$ is Cauchy's stress tensor while ε is the strain tensor. One then needs to find admissible displacement and stress fields $s = (\mathbf{u}, \boldsymbol{\sigma}) \in \mathcal{U} \times \mathcal{S}$ that also satisfy the constitutive relations.

The weak formulation of the dynamic equilibrium then reads

$$-\int_{\Omega \times I} \boldsymbol{\sigma} : \varepsilon(\mathbf{u}^*) d\Omega dt + \int_{\Omega \times I} \mathbf{f}_d \cdot \mathbf{u}^* d\Omega dt + \int_{\partial\Omega \times I} \mathbf{F}_d \cdot \mathbf{u}^* dS dt = \int_{\Omega \times I} \rho \ddot{\mathbf{u}} \cdot \mathbf{u}^* d\Omega dt \quad \forall \mathbf{u}^* \in \mathcal{U}^0. \quad (1)$$

In addition to this dynamic equation, the material behaviour of the structure is described through nonlinear equations which motivates the methodology introduced in this work.

3 DUCTILE DAMAGE MODEL INCLUDING CRACK CLOSURE EFFECT

The damage evolution in the structure is governed by a plastic model [8] with linear kinematic and isotropic hardening along with isotropic damage contribution [9]. In order to account for crack-closure effect, an effective stress tensor $\tilde{\boldsymbol{\sigma}}$ [10] is introduced to read

$$\tilde{\boldsymbol{\sigma}} = \frac{\boldsymbol{\sigma}_d}{1-D} + \left[\frac{\langle \sigma_H \rangle}{1-D} - \langle -\sigma_H \rangle \right] \mathbf{1}, \quad (2)$$

with $\boldsymbol{\sigma}_d$ the deviatoric part of Cauchy's stress $\boldsymbol{\sigma}$ and σ_H its hydrostatic part, D the damage variable, $\mathbf{1}$ the identity tensor and $\langle \square \rangle = \max(\square, 0)$ defining the positive part. Doing so leads to Hooke's relation between stress and elastic strain reading

$$\tilde{\boldsymbol{\sigma}} = \mathbb{K} : \boldsymbol{\varepsilon}^e \quad (3)$$

with \mathbb{K} the Hooke's tensor. Thus, the damage variable is no more explicitly apparent in the elastic constitutive relation.

When the solicitation is high, some non reversibilities appear and plastic laws as well as new variables are required. The yield function $f_p(\boldsymbol{\sigma})$ describes the elastic domain. When the stress is small enough for the function to be negative then the material follows an elastic behaviour but when the yield function increases to the point that it reaches zero, non reversibilities appear and plasticity laws become necessary. The plasticity yield function f_p verifies

$$f_p \leq 0, \quad (4)$$

and is written using von Mises equivalent stress $J_2(\square)$ as follows

$$f_p = J_2 \left(\frac{\boldsymbol{\sigma}}{1-D} - \mathbf{X} \right) - \sigma_y - R \quad (5)$$

with σ_y the yield stress, R the isotropic hardening variable and \mathbf{X} the kinematic hardening tensor.

The model chosen to describe those irreversibilities, following the lines of [8], involves both kinematic and isotropic hardening. The elastic strain tensor reads $\boldsymbol{\varepsilon}^e = \boldsymbol{\varepsilon} - \boldsymbol{\varepsilon}^p$ with $\boldsymbol{\varepsilon}^p$ being the plastic strain. The plasticity level is described by an internal variable called the cumulative plastic strain p which is a strictly increasing quantity. State equations relative to linear hardening read

$$\begin{cases} R = hp, \\ \mathbf{X} = \frac{2}{3}C\boldsymbol{\alpha} \end{cases} \quad (6)$$

with h the rate at which the isotropic hardening increases, C a material coefficient and $\boldsymbol{\alpha}$ the kinematics internal variable.

Lemaitre's damage evolution law reads as a function of the *elastic energy density* Y defined as

$$Y = \frac{1}{2} \boldsymbol{\varepsilon}^e : \mathbb{K} : \boldsymbol{\varepsilon}^e = R_\nu \frac{J_2(\tilde{\boldsymbol{\sigma}})^2}{2E}, \quad (7)$$

where the triaxiality function $R_\nu = \frac{2}{3}(1+\nu) + 3(1-2\nu) \langle \frac{\tilde{\sigma}_H}{J_2(\tilde{\boldsymbol{\sigma}})} \rangle^2$ is introduced.

In order to predict the temporal evolution of these quantities, evolution laws are needed. Plasticity evolution laws are derived using normality rule, leading to

$$\begin{cases} \dot{\boldsymbol{\varepsilon}}^p = \dot{p} \frac{3}{2} \frac{(\tilde{\boldsymbol{\sigma}} - \mathbf{X})_d}{J_2(\tilde{\boldsymbol{\sigma}} - \mathbf{X})}, \\ \dot{\boldsymbol{\alpha}} = \dot{p} (1-D) \left[\frac{3}{2} \frac{(\tilde{\boldsymbol{\sigma}} - \mathbf{X})_d}{J_2(\tilde{\boldsymbol{\sigma}} - \mathbf{X})} \right]. \end{cases} \quad (8)$$

As for the damage variable, the evolution is written as

$$\dot{D} = \dot{p} \left(\frac{Y}{S} \right)^s, \text{ if } W_s > W_D, \quad (9)$$

with W_s the so-called *corrected stored energy* [9], W_D a given energy threshold, s and S material parameters. This set of equations allows to describe finely the damage state evolution of the structure but the resulting problem is nonlinear and involves a large number of degrees of freedom.

4 THE LATIN-PGD

Using the finite element method, the mechanical problem gives a detailed description of the evolution of the quantities of interest but its computation requires solving nonlinear equations at each Gauss point at each given time step. That leads to a high computational cost that could be driven down by using model-order reduction techniques.

4.1 The PGD method

For solving linear problems, the idea of the PGD technique is to look for the solution as the sum of products of single-variable functions. Thus, a displacement field u is approximated by $u_N(\mathbf{x}, t)$ reading

$$u(\mathbf{x}, t) \approx u_N(\mathbf{x}, t) = \sum_{i=1}^N \bar{u}_i(\mathbf{x}) \lambda_i(t). \quad (10)$$

The reduced basis $\{\bar{u}_i\}$ is not a priori known and is built during the computation using a greedy algorithm. New modes are added on the fly. In order to perform a PGD, the used greedy algorithm requires that one solves a linear space-time problem. Hence having a method turning the nonlinear problem into solving linear equations on such a domain is mandatory.

4.2 The LATIN solver

The LATIN method, first introduced in [11] has been singled out as it is an iterative non incremental solver that allows seeking a solution on the entire space-time domain while some of the computations involve linear equations. Each LATIN iteration is decomposed in so-called *local* and *global* stages. At the local stage, the nonlinear part of the constitutive relations is solved at each Gauss point and at the global stage, admissibility is imposed on the whole time-space domain leading to a linear problem. The PGD can be used for an efficient computation of the solution at the linear stage. Those solutions belong respectively to the manifold Γ gathering solutions of the nonlinear equations and the manifold \mathcal{A}_d gathering solutions of the linear equations. The final solution s_{exact} , which is naturally found at the intersection of these two manifolds, is thought alternatively in both spaces \mathcal{A}_d and Γ involving two search directions \mathbb{H}^+ and \mathbb{H}^- linking the manifolds through Eq. (11),

$$\begin{cases} (\boldsymbol{\sigma}_{n+1} - \hat{\boldsymbol{\sigma}}_{n+1/2}) - \mathbb{H}^- (\boldsymbol{\varepsilon}_{n+1} - \hat{\boldsymbol{\varepsilon}}_{n+1/2}) = \mathbf{0}, \\ (\hat{\boldsymbol{\sigma}}_{n+1/2} - \boldsymbol{\sigma}_n) + \mathbb{H}^+ (\hat{\boldsymbol{\varepsilon}}_{n+1/2} - \boldsymbol{\varepsilon}_n) = \mathbf{0}. \end{cases} \quad (11)$$

This iterative scheme can be sketched by Fig. 2 where $\hat{s}_{n+1/2}$ is the solution belonging to Γ and s_{n+1} is a solution of \mathcal{A}_d , both computed at the $(n+1)^{\text{th}}$ stage of the method.

The solution can be initialized to a kinematically and dynamically admissible elastic solution. Then one loops over finding alternatively a solution in Γ and in \mathcal{A}_d until a stopping criterion is reached. Such a criterion is satisfied when an error indicator

$$\eta^2 = \frac{\|\hat{s}_{n+1/2} - s_{n+1}\|^2}{1/2\|s_{n+1}\|^2 + 1/2\|\hat{s}_{n+1/2}\|^2}, \quad (12)$$

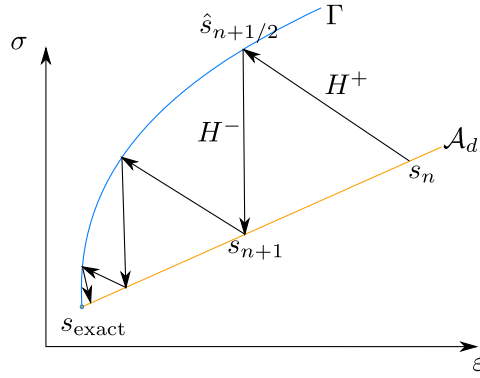


Figure 2: Working principle of the LATIN method, modified from [11]

based on the distance between two consecutive solutions, is lower than a chosen threshold. The norm $\|s\|$ is defined as

$$\|s\|^2 = \int_{\Omega \times I} \boldsymbol{\varepsilon} : \mathbb{K} : \boldsymbol{\varepsilon} \, d\Omega dt + \int_{\Omega \times I} \boldsymbol{\sigma} : \mathbb{K}^{-1} : \boldsymbol{\sigma} \, d\Omega dt. \quad (13)$$

Such a methodology has recently been suggested for a dynamic resolution [7] where the material is considered to be described by a visco-plastic behaviour without considering damage evolution.

4.2.1 The global stage

The global stage consists in finding a solution in \mathcal{A}_d which means solving the dynamic equilibrium defined by Eq. (1). Subtracting that equation written in two successive steps of the LATIN method gives the admissibility equation written in corrective terms reading

$$- \int_{\Omega \times I} \Delta \boldsymbol{\sigma} : \boldsymbol{\varepsilon}(\mathbf{u}^*) \, d\Omega dt = \int_{\Omega \times I} \rho \Delta \ddot{\mathbf{u}} \cdot \mathbf{u}^* \, d\Omega dt \quad \forall \mathbf{u}^* \in \mathcal{U}^0, \quad (14)$$

with $\Delta \square = \square^{n+1} - \square^n$.

To solve that equation the descending search direction given by Eq. (11) is injected in the latter, leading to,

$$\begin{aligned} & \int_{\Omega \times I} \mathbb{H}^- : \boldsymbol{\varepsilon}(\Delta \mathbf{u}) : \boldsymbol{\varepsilon}(\mathbf{u}^*) \, d\Omega dt + \int_{\Omega \times I} \rho \Delta \ddot{\mathbf{u}} \cdot \mathbf{u}^* \, d\Omega dt \\ & = \int_{\Omega \times I} \underbrace{\left[\left(\boldsymbol{\sigma}^n - \hat{\boldsymbol{\sigma}}^{n+1/2} \right) - \mathbb{H}^- : \left(\boldsymbol{\varepsilon}^n - \boldsymbol{\varepsilon}^{n+1/2} \right) \right]}_{-\hat{\mathbf{f}}} : \boldsymbol{\varepsilon}(\mathbf{u}^*) \, d\Omega dt \quad \forall \mathbf{u}^* \in \mathcal{U}^0. \end{aligned} \quad (15)$$

One may notice that terms in the second hand $\hat{\mathbf{f}}$ of that equation are already known quantities. The displacement field is the only unknown.

Because the global stage consists in solving linear equations over the whole time-space domain, a greedy algorithm can advantageously be set up in order to find the solution under a PGD form. To do so, the PGD decomposition $\square(\mathbf{x}, t) = \sum_{i=1}^N \bar{\square}^i(\mathbf{x}) \lambda^i(t)$ of the displacement field is injected into the previous equation to compute the corrections, N being the number of PGD modes used to describe the solution.

4.2.2 The local stage

The local stage consists in solving the local and possibly nonlinear equations of the problem. That means finding $\hat{s}_{n+1/2} \in \Gamma$ knowing $s_n \in \mathcal{A}_d$. The ascendant search direction is chosen vertical, *i.e.* $\hat{\boldsymbol{\varepsilon}}_{n+1/2} = \boldsymbol{\varepsilon}_n$. Technically, the local stage consists in a radial feedback algorithm to compute

the plastic and damage evolution of the structure while taking into account normality law and the von Mises criterion defined by Eq. (4).

5 NUMERICAL RESULTS

In order to illustrate the method, two cases are investigated. First the dynamic aspects of the problem are exposed with a 3D beam under flexion loading. Then a pre-damaged 3D plate with a hole is investigated with various initial damage states. Both geometries are described in Fig. 3 and their dimensions are summarized in Table 1.

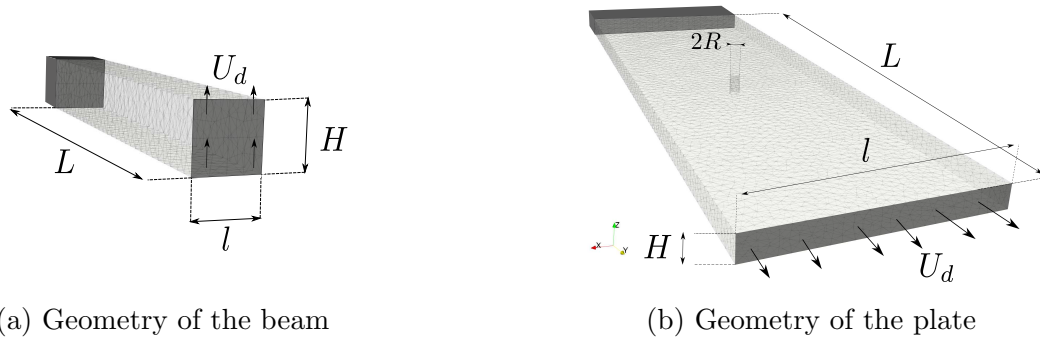


Figure 3: Two test cases geometries

Table 1: Dimensions of the geometries

Geometry	L	l	H	U_d^{\max}	R
Plate	60 mm	20 mm	2 mm	2 mm	1 mm
Beam	40 mm	8 mm	8 mm	5 mm	-

The material parameters are given in Table 2.

Table 2: Material parameters

Name	Parameters
Young's modulus	$E = 200 \text{ GPa}$
Poisson's ratio	$\nu = 0.3$
Kinematic hardening modulus	$C = 2.21 \times 10^4 \text{ MPa}$
Yield stress	$\sigma_y = 200 \text{ MPa}$
Isotropic hardening ratio	$h = 0 \text{ MPa}$
Damage law exponent	$s = 2$
Parameter for damage evolution	$S = 0.6 \text{ MPa}$
Density	$\rho = 7900 \text{ kg/m}^3$
Damage threshold energy	$W_D = 0 \text{ Jm}^3/\text{kg}$

5.1 Dynamic behaviour

A cantilever beam loaded by an imposed vertical displacement U_d at its end, as shown in Fig. 3a, is studied. The beam is submitted to a triangular load for the first half of the simulation then the displacement at the end of the beam is kept equal to zero for the second half. From an initial undamaged state, the damage increases along the beam. The damage maps at $t = 2.5 \times 10^{-4} \text{ s}$,

$t = 6 \times 10^{-4}$ s and $t = 8 \times 10^{-4}$ s are presented in Fig. 4a, 4b and 4c respectively. It can be noted that the first instant corresponds to the maximum amplitude of the external perturbation while the two other instants of interest are posterior to the external load, as shown in Fig. 4d.

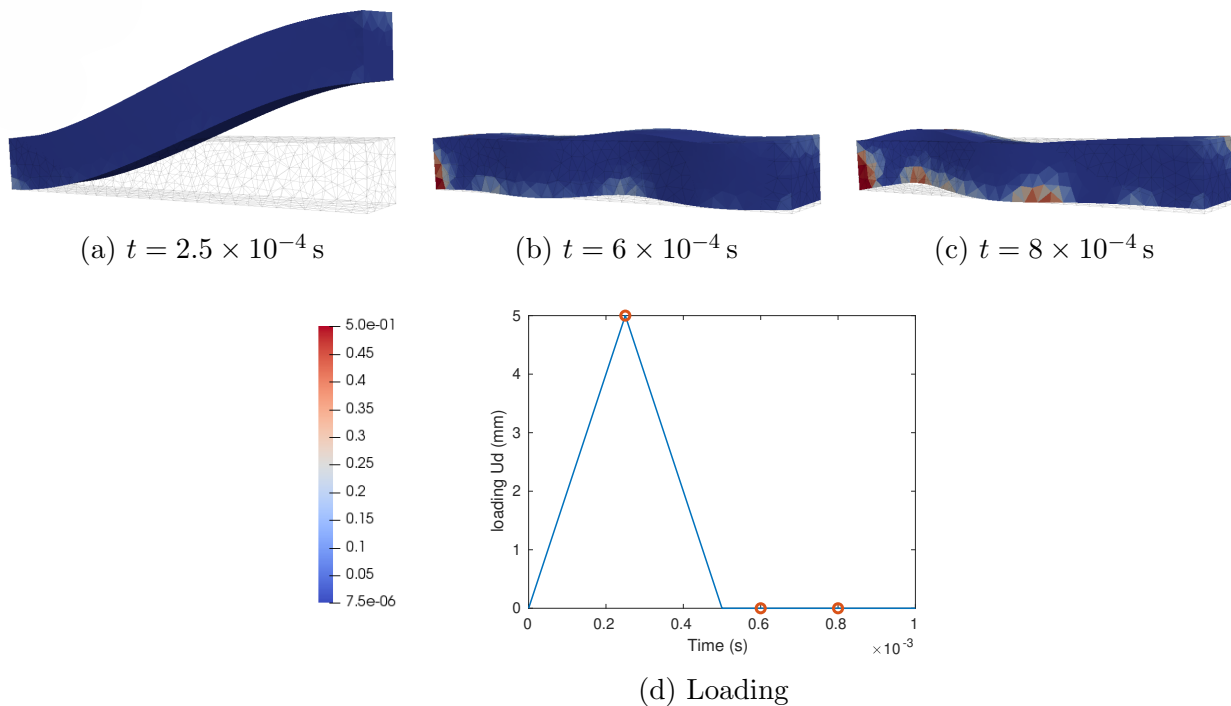


Figure 4: Evolution of the damage map in the beam

One may notice that, even though the last two showcased results (Fig. 4b and 4b) are taken when there is no more external loading, the damage map keeps on progressing. This evolution is therefore only due to inertial forces because waves propagate through the structure as observed in Fig. 4b and Fig. 4c.

The convergence of the LATIN-PGD implementation leading to this result is plotted in Fig. 5 which shows the evolution of the error indicator η with respect to the number of PGD modes. It may be noted that the number of modes is rather large at convergence. Indeed, currently the global stage of the method only consists in adding a PGD mode but a more efficient strategy would be to first update the temporal modes associated with the existing spatial modes and only add a supplementary PGD mode if that update did not prove to be effective enough.

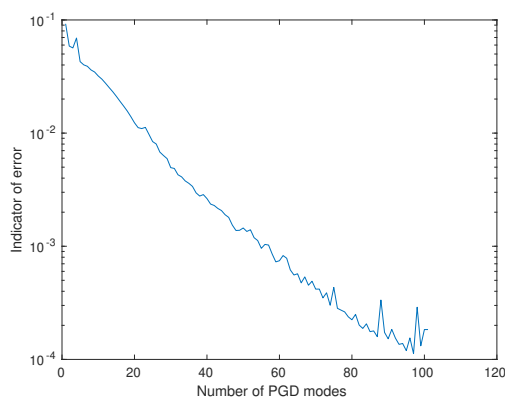


Figure 5: Evolution of the indicator of error for the beam scenario

5.2 Influence of the initial damage state

As previously stated our long term ambition is the construction of virtual charts in which the pre-damage is a parameter. To illustrate the role of a pre-damaged zone on the final solution two simulations with distinct initial damage states have been carried out. The common structure is a plate shown in Fig. 3a and the loading is a 1 s ramp loading directed along the y-axis. The first case scenario (illustrated in Fig. 6a, 6b and 6c) shows the structure with a pre-damaged zone below the hole while the second case scenario (illustrated in Fig. 6d, 6e and 6f) shows the structure with a pre-damaged zone facing the hole. Only a part of the whole structure is shown as to focus on the damaged zones, which are of interest.

When observing the damaged maps projected on the deformed structure in Fig. 6, one can see that damage tends to grow in the surrounding area of the initial damaged zone and near the hole. In the second case scenario similarly damage increases near the hole and the pre-damaged zone first. But a coalescence arises between those two zones. A significant influence of pre-damage zones is therefore observed.

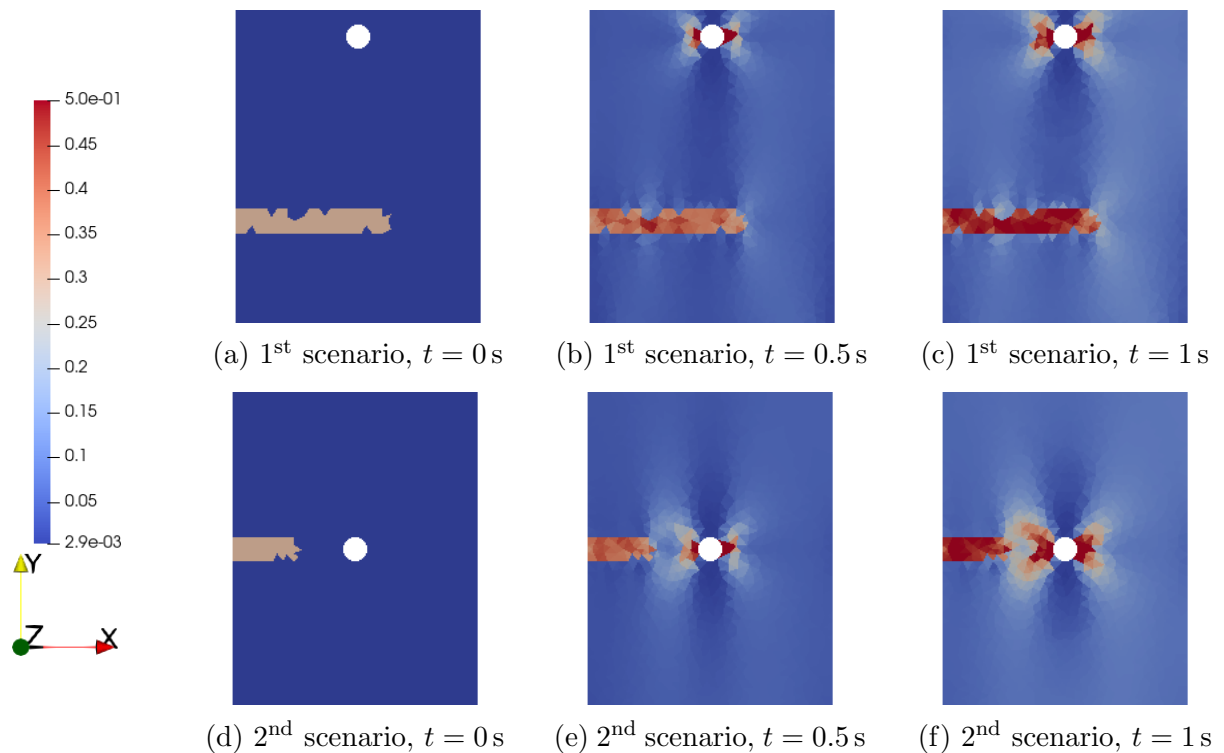


Figure 6: Evolution of the damage map in the plate

As it has been done for the plate, the convergence of the method is plotted in Fig. 7 which shows the evolution of the error indicator η while the number of PGD modes increases. The previous remark about the number of modes at convergence remains valid as a great number of modes is needed here too.

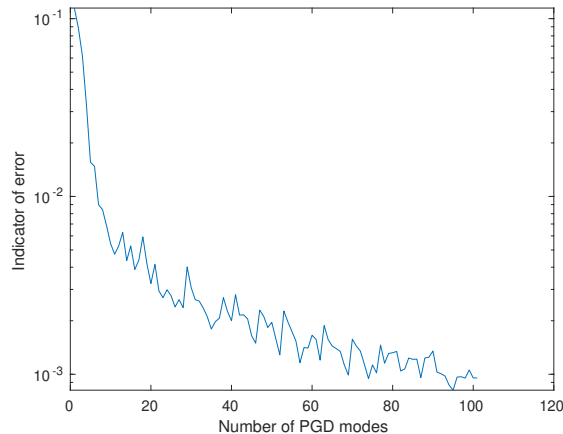


Figure 7: Evolution of the indicator of error for the plate scenario

A few other cases have been implemented showing similar convergence curves, proving the methodology robust enough to investigate a vast variety of scenarii.

6 CONCLUSIONS

The LATIN-PGD framework has been presented for damageable materials in dynamics. Predicting the damage evolution of a plastic structure under a dynamic loading is possible and the computation of the solution gives access to a PGD basis. The next step will be to implement the update strategy in the global stage in order to be able to take advantage of previously computed spatial modes. The LATIN-PGD methodology will then provide a favorable framework for the computation of fragility curves where the seismic performances of quasi-identical structures have to be computed for a family of similar inputs defining the seismic risk. Both initialization of the solution and re-use of reduced order PGD basis enable one to take full advantage of the possible redundancy contained in those virtual charts.

7 ACKNOWLEDGMENT

The SEISM Institute is deeply acknowledged for funding this research activity. This work is hosted by the NARSIS Project that is also thanked for giving the opportunity to study such thematic.

REFERENCES

- [1] T.D Burton and W. Rhee. On the reduction of nonlinear structural dynamics models. *Journal of vibration and control*, 6(4):531–556, 2000.
- [2] M. Kirby, J.-P. Boris, and L. Sirovich. A proper orthogonal decomposition of a simulated supersonic shear layer. *International journal for numerical methods in fluids*, 10(4):411–428, 1990.
- [3] F. A. Lülfi, D.-M. Tran, and R. Ohayon. Reduced bases for nonlinear structural dynamic systems: A comparative study. *Journal of sound and vibration*, 332(15):3897–3921, 2013.
- [4] F. Chinesta, P. Ladevèze, and E. Cueto. A short review on model order reduction based on proper generalized decomposition. *Archives of Computational Methods in Engineering*, 18(4):395–404, 2011.
- [5] P. Ladevèze. *Nonlinear computational structural mechanics: new approaches and non-incremental methods of calculation*. Mechanical engineering series. Springer, New York, 1999.

- [6] D. Néron, P.-A. Boucard, and N. Relun. Time-space PGD for the rapid solution of 3D nonlinear parametrized problems in the many-query context. *International Journal for Numerical Methods in Engineering*, 103(4):275–292, 2015.
- [7] S. Rodriguez, D. Néron, P.-E. Charbonnel, P. Ladevèze, and G. Nahas. Non incremental LATIN-PGD solver for nonlinear vibratory dynamics problems. In *14ème Colloque National en Calcul des Structures, CSMA 2019*, Presqu’Île de Giens, France, May 2019.
- [8] J. Lemaitre and J.-L. Chaboche. Mechanics of solid materials. *Cambridge university press*, 1994.
- [9] J. Lemaitre and R. Desmorat. *Engineering Damage Mechanics: Ductile, Creep, Fatigue and Brittle Failures*. Springer Berlin / Heidelberg, 2005.
- [10] M. Bhattacharyya, A. Fau, R. Desmorat, S. Alameddine, D. Néron, P. Ladevèze, and U. Nackenhorst. A kinetic two-scale damage model for high-cycle fatigue simulation using multi-temporal latin framework. *European Journal of Mechanics / A Solids*, 77, 2019.
- [11] P. Ladevèze. Sur une famille d’algorithmes en mécanique des structures. *Comptes-rendus des séances de l’Académie des sciences. Série 2, Mécanique, physique, chimie, sciences de l’univers, sciences de la terre*, 300(2), 1985.